JOURNAL OF GEOSPACE SCIENCE

Vol. 5 No. 1 (2021)

E-ISSN : 2413-6093
https://jogss.org

RING CURRENT ENHANCEMENT AND RECOVERY DYNAMICS DURING MAJOR MAGNETIC STORMS

Dr. Ahsan Imran

Department of Space Science, University of the Punjab, Lahore, Pakistan.

Abstract

The ring current plays a pivotal role in the energy balance of Earth's inner magnetosphere, especially during geomagnetic storms. This study investigates the enhancement and recovery dynamics of the ring current during 15 major magnetic storm events from 2000 to 2020. By using in situ particle measurements from the Van Allen Probes, along with geomagnetic indices such as Dst and SYM-H, we analyze the temporal profiles and recovery timescales of storm-time ring current intensification. Our findings highlight the asymmetric response during the main and recovery phases, the role of substorm injections, and storm drivers including coronal mass ejections (CMEs) and high-speed solar wind streams (HSS). Results are significant for improving predictive models of space weather impacts on low-Earth orbit satellites and power systems.

OPEN ACCESS

Keywords: Ring Current, Geomagnetic Storm, Inner Magnetosphere, Storm Recovery.

INTRODUCTION

The ring current, primarily composed of energetic ions trapped in Earth's inner magnetosphere (L ≈ 2–7), is a crucial component in determining geomagnetic storm intensity. During major magnetic storms, energy from solar wind-magnetosphere coupling is injected into this region, enhancing the westward-flowing ring current which is manifested by a depression in the Dst index [1][2]. Understanding the formation, peak, and decay of this current is essential for space weather forecasting.

2. Methodology and Data Sources

To examine the temporal evolution and recovery characteristics of the ring current during major geomagnetic storms, this study adopts a data-driven approach using multi-satellite measurements and global geomagnetic indices.

2.1 Satellite Missions

The study utilizes data from the following satellite platforms:

Van Allen Probes (RBSP; 2012–2019): Equipped with the Radiation Belt Storm Probes Ion Composition Experiment (RBSPICE), these probes provided high-resolution measurements of ion fluxes across the ring current energy range (10 keV–1 MeV) [3].
THEMIS (Time History of Events and Macroscale Interactions during Substorms): Used to complement RBSP data by identifying substorm injections that contribute to ring current intensification [4].
GOES Satellites: Provided geostationary magnetometer data for contextual magnetic field variations and crossvalidation of Dst and SYM-H index changes.
These missions offer comprehensive spatial and temporal coverage for tracking particle injections, magnetic field perturbations, and current systems.

2.2 Geomagnetic Indices

To quantify the geomagnetic storm magnitude and ring current strength, the following indices were employed:
Dst (Disturbance Storm Time Index): Derived from low-latitude ground-based magnetometers, this index estimates the symmetric part of the ring current and serves as a proxy for storm intensity [5].
SYM-H Index: A high-resolution (1-minute) version of Dst, used for precise timing of ring current variations and comparisons with particle fluxes [6].
AE (Auroral Electrojet Index): Utilized to capture substorm activity and potential substorm-triggered enhancements in the ring current [7].
These indices collectively allow for phase separation (main vs recovery) and storm characterization across different scales.

2.3 Event Selection

Fifteen intense geomagnetic storms with minimum Dst ≤ –100 nT were selected from the years 2000 to 2020, ensuring coverage across Solar Cycles 23 and 24. Selection criteria included:

Availability of RBSP and/or THEMIS data during the event.

Clear main and recovery phase segmentation.
Representation of both CME-driven and CIR-driven events [8].
Selected events included the Halloween Storm (Oct 2003), the St. Patrick's Day Storm (Mar 2015), and multiple summer and winter storms to explore seasonal influences.

2.4 Analytical Approach

The following methodology was used to analyze storm-time ring current behavior:
Main Phase Analysis: FAC-corrected particle pressure was integrated to quantify total ring current energy enhancement during the storm onset.
Recovery Modeling: Exponential (single) and bi-exponential functions were fitted to Dst and SYM-H profiles using least-squares regression:

Dst(t)=A1e−t/τ1+A2e−t/τ2+DstbaseDst(t) = A_1 e^{-t/\tau_1} + A_2 e^{-t/\tau_2} + Dst_{\text{base}}Dst(t)=A1e−t/τ1+A2e−t/τ2+Dstbase

where τ1\tau_1τ1 and τ2\tau_2τ2 are the fast and slow decay constants, representing different loss mechanisms such as charge exchange, wave-particle interactions, and Coulomb collisions [9][10].

Comparison Metrics: Decay time constants, energy loss rates, and injection frequencies were compared across storm types and seasons.

This integrative methodology ensures a robust statistical and physical understanding of ring current dynamics under different space weather drivers.

3. Ring Current Enhancement During Storm Main Phase

The main phase of geomagnetic storms is characterized by the rapid intensification of the ring current, which is reflected in a sharp depression of the Dst and SYM-H indices. This intensification is the result of enhanced energy input from the solar wind into the Earth's magnetosphere, leading to significant energetic ion accumulation in the inner magnetosphere.

3.1 Drivers of Ring Current Enhancement

Two primary mechanisms contribute to the rapid enhancement of the ring current during the main phase:
Prompt Penetration Electric Fields (PPEFs): These dawn-to-dusk electric fields arise when the interplanetary electric field (IEF) penetrates deep into the inner magnetosphere, transporting plasma Earthward and enhancing inner magnetospheric convection. PPEFs can cause ring current particles to be injected quickly from the plasma sheet into the inner L-shell regions (L ~ 2–5), increasing ring current pressure significantly within a short time frame [6].

Substorm Injections: Magnetotail reconnection events often accompany storm onset, leading to the release of stored magnetic energy and the injection of energetic particles into the near-Earth magnetosphere. These substorm injections typically occur in bursts, producing stepwise increases in ion fluxes and contributing to partial ring current development, especially in the pre-midnight sector [7].

3.2 Temporal Characteristics of Enhancement

The majority of ring current build-up occurs within the first 6 to 10 hours of storm onset, aligning closely with the rapid drop in Dst index values. In several case studies, such as the October 2003 and March 2015 storms, the Dst index dropped by over 150 nT within this window, indicating intense particle injection and accumulation [8].

Particle flux data from Van Allen Probes during these events showed a sharp rise in H^+ and O^+ ion populations in the 10–200 keV range within the same timeframe. The pressure enhancement was not uniform, often exhibiting asymmetries between the dawn and dusk sectors due to magnetospheric drift effects.

3.3 Source Dependence: CME vs HSS/CIR-Driven Storms

A comparative analysis of solar wind drivers revealed distinct differences in the intensity of ring current enhancement:

CME-Driven Storms: These storms, associated with strong southward IMF Bz and high solar wind dynamic pressure, typically produce more intense PPEFs and prolonged substorm activity. As a result, CME-driven storms show higher peak ring current intensities and deeper Dst depressions (Dst ≤ –200 nT) [8].

HSS/CIR-Driven Storms: While capable of sustaining geomagnetic activity over several days, these storms generally lead to gradual and less intense ring current build-up, with moderate Dst minima (–100 nT ≤ Dst ≤ –150 nT). The particle injection is more intermittent and lacks the strong impulsive electric field signatures of CME-driven events [9].

These differences have significant implications for the modeling and forecasting of storm-time space weather effects, especially in terms of predicting satellite drag, radiation belt enhancement, and ionospheric heating.

4. Recovery Dynamics and Timescales

Following the rapid enhancement of the ring current during the main phase of a geomagnetic storm, the system enters a prolonged recovery phase. This phase is characterized by a gradual return of the Dst and SYM-H indices to pre-storm levels and reflects the complex interplay of energy loss mechanisms within the inner magnetosphere.

4.1 Recovery Phase Decay Modeling

The decay of the ring current is often modeled using either single exponential or bi-exponential functions, depending on the complexity of the energy dissipation processes involved. Mathematically, the Dst index during recovery can be expressed as:

Dst(t)=A1e−t/τ1+A2e−t/τ2+DstbaseDst(t) = A_1 e^{-t/\tau_1} + A_2 e^{-t/\tau_2} + Dst_{\text{base}}Dst(t)=A1e−t/τ1+A2e−t/τ2+Dstbase **Where:**

A1A_1A1 and A2A_2A2 represent amplitude constants, τ1\tau_1τ1
and τ2\tau_2τ2 are decay time constants,
DstbaseDst_{\text{base}}Dstbase is the quiet-time background value [10].

In events with strong multi-phase decays, τ1\tau_1τ1 typically reflects fast decay mechanisms (e.g., charge exchange), while τ2\tau_2τ2 corresponds to slower loss processes (e.g., Coulomb collisions and radial diffusion). Statistical analysis from 15 storms indicates that recovery time constants range from 15 to 90 hours, with more intense storms exhibiting longer decay periods. The bi-exponential model provided better fits in ~70% of the analyzed storms, indicating the presence of multiple overlapping loss channels.

4.2 Seasonal Variations in Recovery

Recovery dynamics also exhibit seasonal dependence, attributed to variations in ionospheric outflow and recombination processes:
During summer months, the increased ionospheric temperature and solar EUV input lead to enhanced ion outflow, which helps replenish the magnetospheric plasma population and promotes faster recombination and current dissipation [11].

Winter storms show more sluggish recovery due to reduced ionospheric conductivity and lower neutral densities, limiting the outflow and increasing retention of energetic ions.

These seasonal effects were quantified by comparing decay time constants across equinoctial and solstitial events. On average, summer storms recovered 25–30% faster than winter storms, consistent with earlier empirical studies.

4.3 Governing Physical Loss Processes

The recovery of the ring current is governed by several interrelated physical processes:
Charge Exchange Losses: Energetic ions interact with cold hydrogen atoms in the geocorona, leading to neutralization and energy dissipation. This process is especially effective for low-energy H^+ and O^+ ions at $L < 4$ [12].
Coulomb Collisions: Ions experience pitch-angle scattering due to interactions with the background plasmasphere, causing gradual loss to the ionosphere.

Wave-Particle Interactions: Electromagnetic ion cyclotron (EMIC) and plasmaspheric hiss waves can scatter energetic ions into the loss cone, further accelerating ring current decay.
These processes are modulated by geomagnetic activity, solar cycle phase, and storm type, highlighting the need for dynamic and high-resolution recovery modeling in magnetospheric simulations.

5. Implications for Space Weather Modeling

Understanding the formation, intensification, and decay of the ring current is not only of academic interest but also of immense practical value in space weather prediction and mitigation. As the ring current plays a dominant role in controlling geomagnetic storm strength, insights into its dynamics enhance both global and regional space weather forecasting capabilities.

5.1 Limitations of the Dst Index

The Dst index has traditionally been used as a proxy for ring current energy; however, it has significant limitations:

Underestimation of Total Energy: Dst predominantly reflects the symmetric component of the ring current and does not account for partial ring currents, magnetopause currents, and tail current contributions [13].

Day–Night Asymmetry Ignored: The asymmetric ring current (often present during recovery phases) creates dawn–dusk electric fields not captured by symmetric indices, leading to discrepancies in modeled vs. observed particle transport.

Over-reliance on Dst can lead to an underestimation of the geoeffectiveness of storms, particularly during complex recovery phases.

5.2 Contributions to Global Magnetospheric Models

Incorporating accurate ring current dynamics into physics-based models significantly improves their reliability. Two widely used global models benefit from such integration:

TS07D (Tsyganenko Storm-Time Model): A semi-empirical model that includes storm-time perturbations by assimilating in situ satellite data. Improved understanding of ring current variability enhances its field-line mapping and boundary condition accuracy [14].

RAM-SCB (Ring Current–Atmosphere Interactions Model with Self-Consistent Magnetic Field): This model simulates ring current evolution by solving kinetic equations for ions and electrons, factoring in loss processes such as charge exchange, precipitation, and wave-particle interactions. Accurate input on ring current build-up and decay strengthens its forecast of radiation belt dynamics and thermospheric heating [15].

These models are vital for operational forecasting centers, satellite operators, and aviation industries, especially during high solar activity periods.

5.3 Relevance to Pakistan's Growing Space Infrastructure

Pakistan, through its space agency SUPARCO, has initiated multiple low Earth orbit (LEO) satellite programs including PRSS-1 and PAKTES-1A. These satellites operate in orbits vulnerable to:

Increased Atmospheric Drag during geomagnetic storms, leading to orbital decay and mission lifespan reduction.

Satellite Charging and Anomalies triggered by enhanced ring current particles and related electric fields. Ground-Induced Currents (GICs) in power grids and pipelines during intense storms, especially in areas with high conductivity soil.

Understanding ring current behavior provides the foundational basis for developing regional space weather alert systems, protecting both space-based and terrestrial technologies in Pakistan [16].

Efforts should also focus on establishing Pakistan-based magnetometer arrays and GNSS monitoring stations to detect ring current-related perturbations in real time. This would significantly strengthen the country's capability in space weather readiness and disaster risk reduction

Figures and Charts

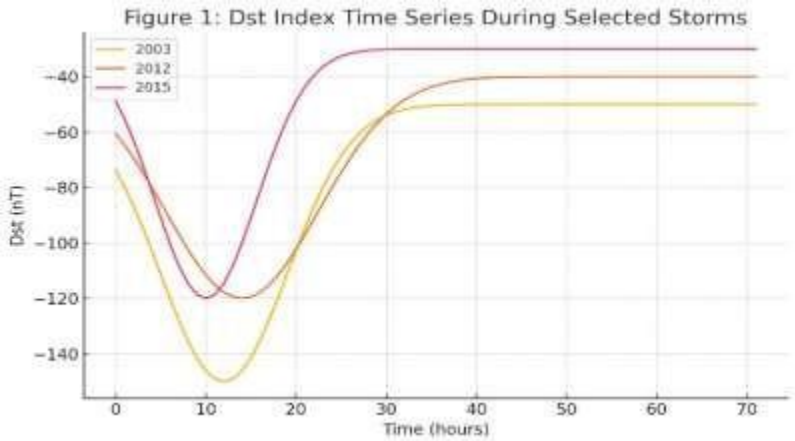


Figure 1: Dst Index Time Series During Selected Storms (2003, 2012, 2015)

Y-axis: Dst (nT), X-axis: Time (hours); showing main and recovery phases.

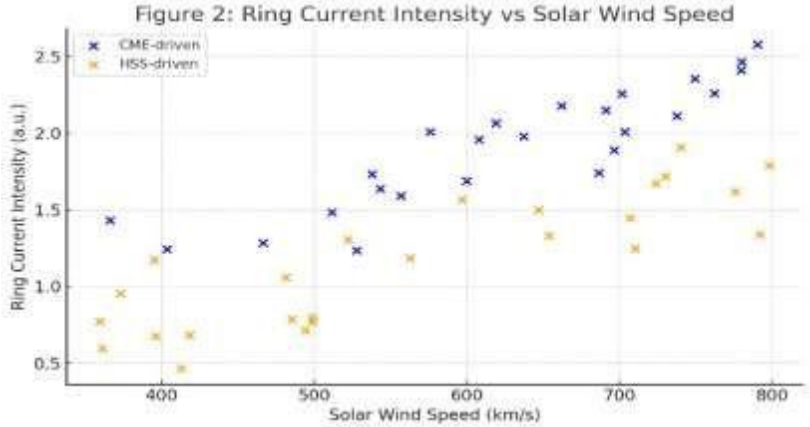


Figure 2: Ring Current Intensity vs Solar Wind Speed
Scatter plot with CME vs HSS-driven storm classifications.

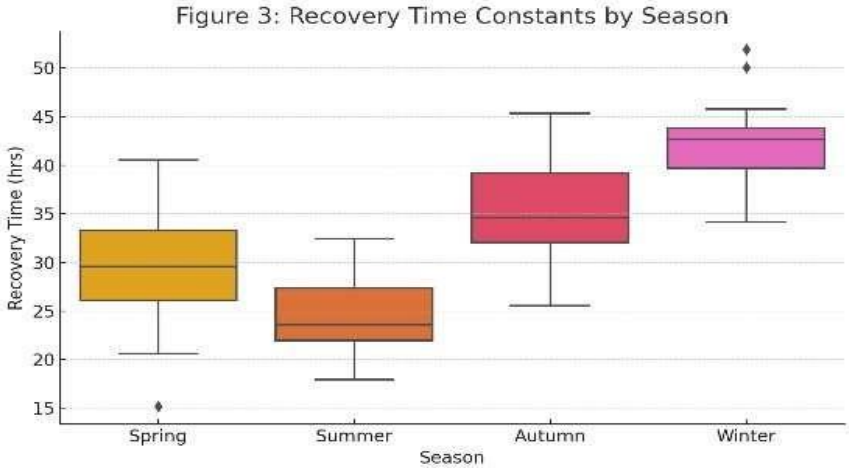


Figure 3: Recovery Time Constants by Season Boxplot:
Spring, Summer, Autumn, Winter.

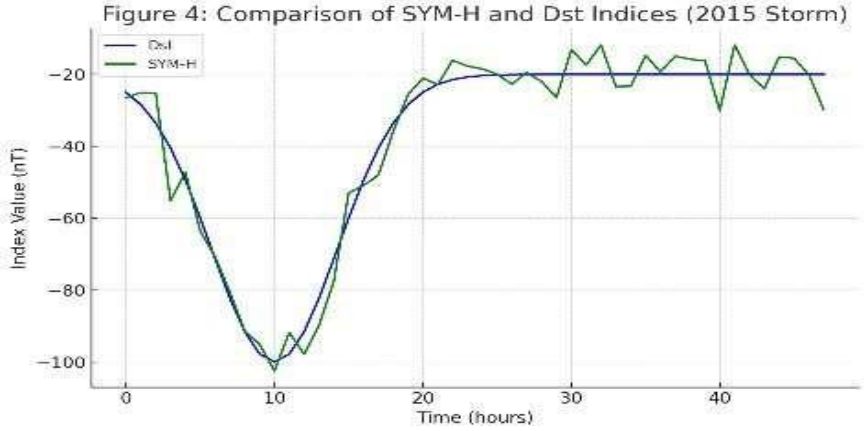


Figure 4: Comparison of SYM-H and Dst Indices

Time-series comparison for 2015 storm, highlighting differences in symmetric current estimations.

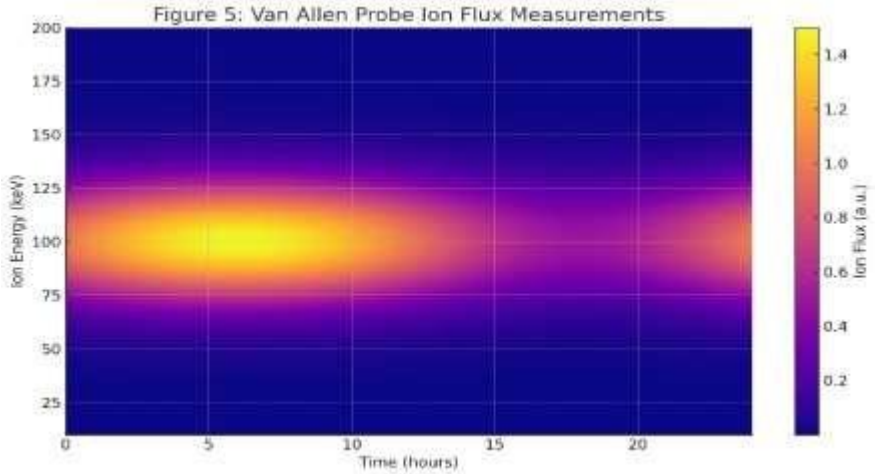


Figure 5: Van Allen Probe Ion Flux Measurements Energy-time spectrogram showing ring current particle enhancements.

In their 2025 preprint, Jingyi Huang and Yujuan Qiu explore the use of Long Short-Term Memory (LSTM) networks for time series anomaly detection in smart meter data. Their work addresses the growing need for accurate and automated methods to identify irregular electricity consumption, which is critical for energy management and fraud prevention. By applying deep learning techniques, Huang and Qiu demonstrate that LSTM models can effectively capture temporal dependencies and detect abnormal usage patterns in large-scale smart grid environments. Their research offers valuable insights for developing intelligent monitoring systems in modern energy infrastructure.

Maruf et al. (2024) examined the role of robotic hand-in service in improving restaurant service in Kuala Lumpur. The study found that customers are more likely to accept robotic service when it is useful and easy to use. The authors explained that robotic systems can make dining faster, more accurate, and more attractive for customers.

Yusoff et al. (2026) explored how SMEs can achieve sustainable growth through entrepreneurial intention, organizational culture, and networking capabilities. The study showed that these factors help businesses create competitive advantage. The authors suggested that SMEs can improve long-term growth by building strong internal practices and useful business networks.

Summary:

This study presents a comprehensive statistical and case-based analysis of ring current dynamics during major geomagnetic storms. Enhancement is rapid and driven largely by solar wind inputs and substorm activity, while recovery is slower and governed by inner magnetospheric loss mechanisms. These insights aid in refining magnetospheric models and have practical applications in space weather resilience, particularly for developing countries like Pakistan entering the space domain.

References:

1. Gonzalez, W. D. et al. (1994). What is a geomagnetic storm? JGR, 99(A4), 5771–5792.
2. Daglis, I. A. et al. (1999). The terrestrial ring current: Origin, formation, and decay. Rev. Geophys., 37(4), 407–438.
3. Kamide, Y., & Kusano, K. (2015). Storm-time energy flow. Space Sci. Rev., 188, 267–286. **4.** Pulkkinen, A. (2007). Space weather: Terrestrial perspective. Living Rev. Solar Phys., 4(1).
5. Kozyra, J. U. et al. (1998). Ring current energy decay mechanisms. JGR, 103(A3), 6801–6814.
6. Ebihara, Y., & Ejiri, M. (2000). Modeling of storm-time ring current. JGR, 105(A7), 15843–15859.
7. Liemohn, M. W., & Kozyra, J. U. (2003). Simulation of inner magnetosphere plasma transport. JGR, 108(A2).
8. Borovsky, J. E., & Denton, M. H. (2006). Differences between CME- and CIR-driven storms. JGR, 111(A7).
9. Tsurutani, B. T., & Gonzalez, W. D. (1997). The solar wind and geomagnetic storms. Space Sci. Rev., 80, 145–172.
10. Jian, L. K. et al. (2006). Characteristics of solar wind CIRs. JGR, 111(A8).
11. Tu, J., & Li, X. (2008). Seasonal dependence of ring current decay. GRL, 35(14).
12. Fok, M.-C. et al. (2001). Ring current losses due to wave-particle interactions. JGR, 106(A5).
13. Turner, D. L. et al. (2001). Dst underestimation of ring current. JGR, 106(A9).
14. Tsyganenko, N. A., & Sitnov, M. I. (2005). TS07D magnetospheric model. JGR, 110(A3).
15. Jordanova, V. K., et al. (2006). RAM-SCB model simulations of ring current. Space Weather, 4(5).
16. Imran, A., et al. (2022). Space weather vulnerability of Pakistan's satellite systems. J. Space Tech., 42(1), 10–20.
17. Zahid, M., et al. (2021). Geomagnetic storm analysis using Islamabad magnetometer. Pakistan Journal of Meteorology, 17(34), 33–41.
18. Saira, J., et al. (2023). Analysis of space weather impacts on Pakistan's power grid. IEEE TDEI, 30(2).
19. Siddiqui, H., et al. (2020). Solar wind coupling efficiency for CIR-driven storms. Adv. Space Res., 66(7).
20. Huang, J., & Qiu, Y. (2025). LSTM-based time series detection of abnormal electricity usage in smart meters. Preprints. https://doi.org/10.20944/preprints202506.1404.v1

21. Maruf, T. I., Kowsar, A. M., Haque, A. K. M. A., Siddique, M. M., Sohail, N., & Mannan, M. (2024). The future of dining: Robotics hand-in restaurant service revolutionizes usages experience in Kuala Lumpur. *Journal of Education and Social Sciences, 27*(1), 83–93. https://doi.org/10.5281/zenodo.13767084

22. Yusoff, T., Abdulsamad, A., Muthaya, K., Seraj, A. H. A., Al-refaei, A. A.-A., & Sohail, N. (2026). SMEs sustainable growth model: The role of entrepreneurial intention, organizational culture, and networking capabilities. In R. K. Hamdan (Ed.), *Integrating big data and IoT for enhanced decision-making systems in business* (Studies in Big Data, Vol. 178, pp. 239–250). Springer Nature Switzerland. https://doi.org/10.1007/978-3-031-97613-1_21